

# 1 The effect of water repellency on the short-term release of CO<sub>2</sub> upon 2 soil wetting

3

## 4 Abstract

5 The spike in carbon dioxide (CO<sub>2</sub>) observed after rewetting of dry soils, known as the 'Birch effect',  
6 can contribute substantially to total soil carbon (C) emissions, however, the exact mechanisms and  
7 timings underlying this sudden CO<sub>2</sub> release remain unclear. The amount of applied water and  
8 duration of the previous dry period are considered the main factors affecting the magnitude of the  
9 CO<sub>2</sub> peak, but the preceding change in soil wettability, triggered by low soil water content, could also  
10 be an important contributor.

11 We investigated the effect of soil water repellency (SWR, assessed by water drop penetration time  
12 test) on the short-term release of CO<sub>2</sub> upon wetting of dry soils with different water quantities. The  
13 experiments were conducted under laboratory conditions using homogeneous and autoclaved soil  
14 from two locations in South Wales (UK) in both wettable and extremely water-repellent states. The  
15 CO<sub>2</sub> efflux was measured using chambers above and below the samples. Upon wetting, CO<sub>2</sub> efflux  
16 was up to 10 times lower in water-repellent soils as a result of rapid percolation through preferential  
17 pathways, with only a small amount of water (up to 10%) retained in the soil. Total CO<sub>2</sub> efflux was  
18 proportional to the water retained in the soil after infiltration, suggesting that the release of CO<sub>2</sub>  
19 occurred only from limited pore-spaces of the soil. The quick CO<sub>2</sub> release suggests that chemical or  
20 biochemical processes, rather than microbial respiration, is the main source of CO<sub>2</sub> efflux in this  
21 study. Part of the CO<sub>2</sub> released was transported to the bottom chamber, which under natural  
22 conditions could enhance the entrapment of gas in the subsoil. This study shows that alterations in

23 the water-filled pore-space as a result of SWR significantly reduced the CO<sub>2</sub> efflux upon wetting and  
24 suggests that SWR could be a key factor when investigating and predicting C fluxes.

25

26 Keywords: hydrophobicity, Birch effect, CO<sub>2</sub> pulse, C emissions, soil degassing, rain pulses

27

## 28 Highlights

- 29 • Low CO<sub>2</sub> pulse in water-repellent soils compared to high pulse in wettable soils.
- 30 • Less than 10% of total water applied retained in water-repellent soils.
- 31 • Total flux was controlled by the amount of water retained in the soil after wetting.
- 32 • Flux transported downwards might contribute to air entrapment deeper in the soil.

33

## 34 1. Introduction

35 Rewetting of dry soils is associated with a large pulse of carbon dioxide (CO<sub>2</sub>) commonly known as  
36 the 'Birch effect' (Birch, 1958). The overall contribution of these short-lived but high magnitude  
37 spikes of CO<sub>2</sub> to the total soil carbon (C) flux could be large (Leon et al., 2014; Smith et al., 2017),  
38 especially with increased frequency and duration of dry spells, which are becoming more common  
39 with the climatic change (Coumou and Rahmstorf, 2012; Trenberth et al., 2013). Although the 'Birch  
40 effect' has been studied for over 50 years, there is still a lack of consensus about the exact causes  
41 and factors affecting the size and duration of the CO<sub>2</sub> pulse (Fraser et al., 2016; Waring & Powers,  
42 2016) which are still not included in the global terrestrial C emissions models (Moyano et al., 2013).

43 Many studies suggest that the 'Birch effect' originates mainly from a quick restoration of microbial  
44 respiration, which is very low in dry soils due to restricted water availability for microorganisms and  
45 the disconnection of soil pores (Borken and Matzner, 2009). After rainfall, the sudden input of water  
46 reconnects the pore system and mobilizes previously unavailable C (Kim et al., 2012; Schimel, 2018)

47 resulting in a boost of microbial activity and a spike in soil CO<sub>2</sub> efflux. The size of the CO<sub>2</sub> pulse is  
48 expected to increase with the amount of water added (Lado-Monserrat et al., 2014; Muhr and  
49 Borken, 2009; Sponseller, 2007). Although the boost in microbial respiration is probably the largest  
50 contributor of CO<sub>2</sub> to the 'Birch effect', some studies argue that the lag period between the wetting  
51 and the reactivation of microbial activity can last several hours (Meisner et al., 2017). It has,  
52 therefore, been suggested that the degassing of soil might be the main contributor of the CO<sub>2</sub> pulse  
53 during the early post-wetting phase (Kim et al., 2012; Norman et al., 1992). Soil gas is not always  
54 emitted immediately. Degassing of CO<sub>2</sub> stored in the pore-space can make up a substantial fraction  
55 of the total CO<sub>2</sub> response to wetting during extreme rainfall events (Maier et al., 2010; 2011;  
56 Huxman et al., 2004; Inglima et al., 2009; Liu et al., 2002).

57 'Birch effect' studies have focussed mainly on the duration and intensity of the drought (de Nijs,  
58 2018; Göransson et al., 2013; Meisner et al., 2015), precipitation rates (Lado-Monserrat et al., 2014;  
59 Muhr et al., 2008) or the type of wetting (Smith et al., 2017) as the main factors affecting the size of  
60 the pulse. In a recent study (Sánchez-García et al., 2020) we have shown that restricted infiltration,  
61 caused by soil water repellency (SWR), can also alter the CO<sub>2</sub> efflux response to wetting  
62 substantially. SWR is a transient property of many soils, especially those under permanent (Doerr et  
63 al., 2000) and stress-tolerant vegetation at low soil water content (SWC) (Seaton et al., 2019). SWR is  
64 primarily caused by the coating of soil particles by hydrophobic organic compounds and can become  
65 especially severe after dry periods or fires (DeBano, 2000; Doerr & Thomas, 2000). Current changing  
66 climate conditions resulting in higher incidence and intensity of droughts will likely enhance the  
67 occurrence and severity of SWR (Goebel et al., 2011). By inducing changes in soil microbial  
68 properties and community structure in response to environmental stressors like drought, soils with  
69 stress-tolerant vegetation can develop hydrophobic layers in order to adapt to low water availability  
70 (Seaton et al., 2019). Thus many soils subjected to dry spells change their hydrological properties by  
71 developing this lack of wettability. Robinson et al. (2019) highlighted the need to incorporate the  
72 dynamics of hydraulic properties in response to such biological feedbacks.

73 Water-repellent soils do not allow free infiltration of water; instead, water either runs off the  
74 terrain's surface (Doerr et al., 2003) or beads up and percolates quickly into the subsoil through  
75 preferential flow paths, leaving much of the topsoil dry (Doerr et al., 2000; Ritsema and Dekker,  
76 1994). The infiltration patterns of water-repellent soils are thus substantially different to wettable  
77 ones, and therefore, the CO<sub>2</sub> efflux in response to wetting of such soils is unlikely to be the same.  
78 Despite this, evidence of water repellency-induced changes in soil C dynamics remains sparse. A few  
79 studies have focused on respiration rates in water-repellent soils (Goebel et al., 2007; Lamparter et  
80 al., 2009) or the overall effects of SWR on CO<sub>2</sub> fluxes (Urbanek and Doerr, 2017) rather than on  
81 short-term spikes of CO<sub>2</sub> after rainfall events. In a previous study, (Sánchez-García et al., 2020) we  
82 presented evidence that SWR reduces the CO<sub>2</sub> pulse after wetting of soil; however, the effect of the  
83 rewetting rate on the magnitude and the duration of the CO<sub>2</sub> pulse in water-repellent soils have  
84 remained unclear.  
85 In this study we address this research gap and aim to improve understanding of the effect of SWR on  
86 the CO<sub>2</sub> efflux upon rewetting. We hypothesise that i) the amount of released CO<sub>2</sub> is proportional to  
87 the rewetting rate of the soil and ii) the initial CO<sub>2</sub> pulse can be mainly caused by the physical release  
88 of gas present in soil pores by infiltrating water rather than a spike in microbial activity.

89

## 90 2. Research design and methods

91 This study involves a series of wetting experiments on homogenised soil under laboratory  
92 conditions. Soil material used for the experiments was autoclaved to remove the contribution from  
93 microbial respiration to CO<sub>2</sub> fluxes and to isolate the physical release of CO<sub>2</sub>, but also to obtain soils  
94 with contrasting wettability that otherwise have similar physico-chemical properties (Urbanek et al.,  
95 2010). Autoclaving of dry or very wet soils keeps the soils wettable, while at intermediate water  
96 content prior to autoclaving the soil turns water-repellent. All soil samples were subjected to one  
97 single wetting treatment applied from above to simulate a rainfall event. CO<sub>2</sub> fluxes were monitored  
98 above and below the soil sample in order to capture CO<sub>2</sub> movement upwards and downwards.

## 100 2.1. Soil sampling and preparations

101 Soil was collected from two locations in the Gower peninsula in South Wales (UK): a sandy loam  
102 referred to as Cefn Bryn (CB) (51° 35'N, 4° 10'W) and a loamy sand referred to as Southgate (SG) (51°  
103 33'N, 4° 5'W) (Table 1). Soils at both locations are under natural grasslands with occasional animal  
104 grazing. The selected soils were used in previous studies (Urbanek et al., 2010; Gazze et al., 2017)  
105 and were known to develop SWR under natural conditions. The use of two types of soil material of  
106 different texture and SOM content allowed us to examine to what degree similar behaviour is  
107 observed in water-repellent soils despite differences in their physico-chemical properties.

108 Soil material was collected from approximately the top 2 to 10 cm over an area of 2 m<sup>2</sup>, after careful  
109 removal of the grass root layer, brought to the laboratory, and air-dried and sieved to 2 mm. In  
110 order to prepare soil material of the same physico-chemical properties, but contrasting wettability,  
111 soil was pre-treated using a technique developed by Urbanek et al. (2010), which involved  
112 autoclaving the soil material at different SWC to obtain wettable and water-repellent soil. In order to  
113 determine an optimal SWC that results in the most contrasting wettability, a small sample of each  
114 soil at air dry, 10, 15, 40 and 50% SWC (grav.) was autoclaved (121 °C for 1 h) followed by oven-  
115 drying at 25 °C for 24 h to achieve similar SWC across all the samples (see Table 2 for a full range of  
116 results). Soil wettability was measured before and after autoclaving using the water drop  
117 penetration time (WDPT) test by placing 5 drops of water on the smoothed surface of a sample and  
118 categorised into the following classes (Doerr, 1998): wettable (< 5 s), slightly repellent (5–60 s),  
119 moderately repellent (60–600 s), strongly repellent (600–3600 s) and extremely repellent (> 3600 s).  
120 Based on these tests, SWC for autoclaving was chosen to be 15% for both CB and SG soils to obtain  
121 extreme SWR (thereafter called CB-WR and SG-WR), and for the wettable soil 40% and 50% SWC was  
122 used for CB and SG respectively (thereafter called CB-NWR and SG-NWR). Although WDPT does not

123 detect small variations in subcritical water repellency (Urbanek et al., 2007; Goebel et al., 2012), in  
124 this case WDPT was suitable given the contrasting wettability between our samples.

125 Other basic soil properties of the two soil materials were determined using standard methods; pH  
126 using a pH electrode in 1:5 dilutions of distilled water and CaCl<sub>2</sub>, soil organic matter (SOM) using the  
127 loss of ignition method (Nelson and Sommers, 1996), particle size distribution using the laser  
128 diffraction method (LS230 laser particle size analyser, Beckman Coulter, Brea, CA) and particle  
129 density ( $\rho$ ) following the Gay-Lussac Specific-Gravity Bottles method (Wofford and Vidrio, 2015  
130 adapted). SWC was determined gravimetrically by moisture loss (105 °C, 24 h).

131

## 132 2.2. Soil wetting and CO<sub>2</sub> efflux measurements

133 Dry sterile soil at respective wettability (wetable and water-repellent) was packed into cylinders  
134 (8 cm diameter, 5 cm height) at bulk densities representative of field conditions: 1.16 and 0.82 g cm<sup>-3</sup>  
135 for CB and SG respectively. The repacked cylinders were rewetted from above using a custom-made  
136 rainfall simulator fitted between the soil sample collar and the CO<sub>2</sub> flux chamber (Fig. 1). The rainfall  
137 simulator comprised one spiral tube with uniformly distributed drips, to ensure spatially uniform  
138 wetting, suspended 1 cm above the soil surface and connected via a tube to a large syringe to supply  
139 water. All cylinders received one single and uniform wetting application with water at an intensity of  
140 100 mm h<sup>-1</sup> to simulate a heavy rainfall event. The applied water was equivalent to 25, 50, 75 and  
141 100% of water-filled pore-space (WFPS). WFPS for each soil was calculated by dividing  
142 volumetric water content by pore-space (PS) and pore-space was obtained from bulk density (dB) as  
143 follows:  $PS = (1 - dB d_p^{-1}) \times 100$ ; assuming a particle density ( $d_p$ ) = 2.65 g cm<sup>-3</sup> (Blake, 2008). After  
144 wetting, water retained in the soil sample was quantified via the weight difference in the soil before  
145 and after wetting.

146 Each cylinder was suspended on a set of collars allowing monitoring of CO<sub>2</sub> concentration in  
147 the chamber above and below the sample simultaneously during the wetting and collection of

148 drained water in the container below (Fig. 1). CO<sub>2</sub> concentration was monitored via a 10 cm  
149 survey chamber connected to an infrared CO<sub>2</sub> gas analyser system (IRGA) from above (Li-8100A, Li-  
150 COR Inc., Lincoln, NE) and a plastic container of a similar headspace connected to a separate  
151 IRGA CO<sub>2</sub> analyser system below the sample referred to as 'bottom chamber' (Li-8100A, Li-COR Inc.,  
152 Lincoln, NE). A fine mesh was placed under the cylinders to allow any drainage of water while  
153 holding the soil inside the cylinder. The entire system (chambers, rainfall simulator and soil sample)  
154 was sealed to avoid gas leakage. The chamber's inbuilt pressure vent maintained ambient pressure  
155 inside the chamber (Fig. 1). The total time of post-wetting CO<sub>2</sub> fluxes monitoring was 150 min, the  
156 gas chamber remained closed for 30 min and vented for 1 min prior to the next closure.

157 The CO<sub>2</sub> concentration data obtained was fitted to a single-term exponential model, excluding the  
158 first 30 s of measurements, which is the typical time required to achieve steady mixing inside  
159 the chamber (LICOR, 2010). The following equation (Eq. 1) was applied to calculate CO<sub>2</sub> flux as the  
160 rate of change in CO<sub>2</sub> concentration released from soil (LICOR, 2010):

161 Eq. 1 
$$FC = \frac{10VPo}{RS(To+273.15)} * \frac{dC'}{dT}$$

162

163 Fc = soil CO<sub>2</sub> efflux (μmol m<sup>-2</sup>s<sup>-1</sup>), V = volume (cm<sup>3</sup>), Po = initial pressure (kPa), S = soil surface  
164 area (cm<sup>2</sup>), To = initial air temperature (°C) and dC'/dT = initial rate of change in water-corrected CO<sub>2</sub>  
165 mole fraction (μmol mol<sup>-1</sup>). The CO<sub>2</sub> flux data below R<sup>2</sup> ≥ 0.95 was rejected with a total of 10 and 15%  
166 of total rejected measurements above and below the sample respectively. The CO<sub>2</sub> flux graphs  
167 were created by calculating the mean flux (n = 3) for each treatment at each measurement time  
168 along with 95% confidence intervals. The Mann-Whitney U-Test was applied to test for statistical  
169 differences (accepted at p < 0.05) between wettable and water-repellent soils.

170

## 171 3. Results

### 172 3.1. CO<sub>2</sub> efflux before and after wetting

173 The CO<sub>2</sub> efflux from dry soils prior to wetting was very low. In all soils, the efflux measured in the top  
174 chamber was below 1  $\mu\text{mol m}^{-2} \text{s}^{-1}$  and negligible in the bottom chamber (Fig. 2 and 3). The CO<sub>2</sub>  
175 efflux increased immediately in response to the wetting, which began exactly 20 min after the initial  
176 start of the observation. A clear increase in CO<sub>2</sub> efflux occurred in all wettable soils, with the  
177 maximum value observed during the wetting period for most samples, or immediately after the  
178 wetting period for SG-NWR with 25 and 50% rewetting rates. Fluxes in the wettable soils peaked 1  
179 and 5 min after the start of wetting for CB and SG respectively. Under wettable conditions, large  
180 differences in the size of the pulse were observed between CB and SG soils with similar amounts of  
181 water added. In the CB-NWR soil the efflux peaks ranged between 5–7  $\mu\text{mol m}^{-2} \text{s}^{-1}$ ; whereas for SG-  
182 NWR soil, peak values were lower, ranging between 2.5–3.5  $\mu\text{mol m}^{-2} \text{s}^{-1}$ . The larger amount of water  
183 added to the soil resulted in a longer duration of the peak, but did not affect the peak size. Overall,  
184 the size of the peak was higher but consistently shorter in CB soil, lasting between 11 and 20 min  
185 depending on the rewetting rate. For instance, doubling the rewetting rate from 25 to 50% increased  
186 the duration of the pulse by 4 min in both CB and SG soils, but no differences in the duration of the  
187 pulse were observed in SG soils with rewetting rates above 50%. In CB soils, the duration of the  
188 pulse increased by 4 min with a 75% rewetting rate but remained similar with a 100% rewetting rate.

189 The differences in the CO<sub>2</sub> efflux between wettable and water-repellent soils were very distinct. In  
190 both CB-WR and SG-WR, the size of the CO<sub>2</sub> pulse in the top chamber was up to ten times lower than  
191 in the corresponding wettable soils ( $p < 0.001$  for both CB and SG soils). Peak sizes in water-repellent  
192 soils ranged from 1 to 3  $\mu\text{mol m}^{-2} \text{s}^{-1}$  in the CB-WR, but in the SG-WR the CO<sub>2</sub> efflux hardly changed  
193 as a result of wetting (peak size 0.3 to 0.6  $\mu\text{mol m}^{-2} \text{s}^{-1}$ ). During the wetting of CB-WR, a distinct  
194 double peak was observed with rewetting rates above 50%. By the end of the observation period, at



195 145 min after the start of wetting, the CO<sub>2</sub> fluxes returned to pre-wetting values and no significant  
196 differences were observed between soils of contrasting wettability ( $p = 0.229$ ).

197 Prior to wetting, the CO<sub>2</sub> flux in the bottom chamber, which represented the amount of CO<sub>2</sub> diffused  
198 downwards the soil profile, was low in both wettable and water-repellent soils. In CB-WR, CO<sub>2</sub> fluxes  
199 did not increase with the start of the wetting in the bottom chamber; instead, a pulse was observed  
200 towards the end of the wetting period. Similar to the top chamber, no CO<sub>2</sub> flux response was  
201 observed in SG-WR; whereas, in the SG-NWR soil, CO<sub>2</sub> fluxes increased with the beginning of wetting  
202 and a significantly higher pulse than in the water-repellent soil was observed ( $p < 0.001$ ). No  
203 significant differences were observed between the pulses in the top and bottom chambers in both  
204 CB-WR and SG-WR ( $p = 0.525$  and  $p = 0.184$  respectively); however, the CO<sub>2</sub> pulses were higher in  
205 the top than in the bottom chamber for both CB-NWR and SG-NWR ( $p = 0.001$  and  $p < 0.001$   
206 respectively).

207

### 208 3.2. Cumulative CO<sub>2</sub> efflux

209 The cumulative CO<sub>2</sub> efflux, calculated as the total CO<sub>2</sub> flux from both the top and bottom chambers  
210 combined, increased with the rewetting rate in wettable soils. The more water that was added to  
211 the soil, the higher the cumulative efflux was in the CB-NWR soil. In the SG-NWR, the cumulative  
212 efflux with the higher rewetting rates ( $\geq 50\%$ ) was very similar, but in contrast, the cumulative efflux  
213 at the lowest rewetting rate (25% WFPS) was significantly lower. In water-repellent soils, the  
214 cumulative efflux from both CB and SG soils was significantly lower ( $p < 0.01$  for both CB and SG)  
215 than in the corresponding wettable soils, except in the CB soil with 25% rewetting rate (Fig. 4). The  
216 cumulative CO<sub>2</sub> efflux increased only slightly, but not significantly, with rewetting rates above 50% in  
217 CB-WR. In SG-WR, the cumulative efflux was similar independently of the rewetting rate; only at 25%  
218 rewetting rate was the cumulative efflux lower, but not significantly, than for the rest of rewetting  
219 rates.

220 In wettable soils, the cumulative CO<sub>2</sub> efflux was positively correlated to the water retained in the soil  
221 after wetting (Fig. 5). In the CB-NWR soil, a positive relationship between the cumulative CO<sub>2</sub> efflux  
222 and the amount of water retained in the soil after wetting was observed, but a surprisingly large  
223 efflux was observed in CB-WR with only a small amount of water retaining in the soil. For example,  
224 8 cm<sup>3</sup> of retained water resulted in cumulative efflux of 5.8 mmol m<sup>-2</sup>, a value similar to those  
225 observed in the wettable soils where more than 90% of water was retained in the soil after the  
226 wetting.

227

### 228 3.3 Effect of SWR on wetting, drainage and retained water

229 Soils of contrasting wettability (wetable WDPT < 5 s; extremely water-repellent WDPT > 3600 s)  
230 showed a very different response to wetting. All the water applied during the rainfall simulations  
231 infiltrated eventually into the soil, but for the wettable soils the infiltration was instant  
232 (WDPT < 5 s), while for the water-repellent soils, the average WDPT infiltration times were 7312 s  
233 and 10368 s for CB-WR and SG-WR respectively (Table 2). For the wettable soils, over 90% of the  
234 water added was retained in the soil, with only a small fraction of it draining to the container below  
235 the soil sample. In contrast, for the water-repellent soils, a significantly lower fraction of the total  
236 water applied (up to 6 and 10 % in the CB-WR and SG-WR respectively) was retained in the soils  
237 ( $p < 0.001$  for both soils), with the remaining 94 to 90%, respectively, draining out of the soils (Table  
238 3). Following wetting, SWC significantly increased accordingly with the rewetting rate in wettable  
239 soils, but in water-repellent soils, only small and non-significant differences were observed between  
240 different rewetting rates in CB and SG soils. An exception was SG-WR with 25% rewetting rate where  
241 SWC was significantly smaller than with the rest of rewetting rates.

242

#### 243 4. Discussion

244 A distinctively lower CO<sub>2</sub> efflux response to the simulated rainfall was observed in the water-  
245 repellent soils compared to the typical 'Birch effect' seen in the wettable soils. Limited water  
246 infiltration and percolation patterns, characteristic of water-repellent soils, affected not only soil  
247 hydrology, but also led to reduced CO<sub>2</sub> efflux. SWR delays and limits infiltration of water to specific  
248 pathways of higher wettability or macropores created by roots, cracks, stones (Urbanek and  
249 Shakesby, 2009; Urbanek et al., 2015) and can result in rapid percolation of water downward to the  
250 subsoil via preferential flow paths (Ritsema and Dekker, 2000; Müller et al., 2014). Water typically  
251 travels in water-repellent soils through a narrow cross-section of soil pores, which results in the  
252 majority of the soil matrix remaining dry after rainfall (Hendrickx and Flury, 2001). Such rapid  
253 percolation through the water-repellent soil was also observed in this study. The water travelled  
254 only through a small fraction of the soil pores and within a short period of time (2 min of the start of  
255 wetting), up to 95% of the water applied drained into the container below the sample. The amount  
256 of water retained in the soil after wetting was minimal, with SWC ranging between 2–6% (Table 3).  
257 Only slight increases in the SWC were observed when higher amounts of water were applied,  
258 suggesting that the water moved through similar cross-sections of the pore-space regardless of the  
259 amount added to the surface. We expect that, in the water-repellent soils, infiltrating water released  
260 the soil CO<sub>2</sub> only from the affected sections of the soil matrix, resulting in the low CO<sub>2</sub> efflux  
261 observed in the headspace of the top and bottom chambers (Fig. 2 and 3). In contrast, in wettable  
262 soils, the large CO<sub>2</sub> pulse observed is likely to have resulted from the relatively uniform infiltration of  
263 water, which released the CO<sub>2</sub> out of the whole cross-section of the soil matrix (Fig. 6). Over 95% of  
264 the applied water was retained in the wettable soils. The more water that was applied, the higher  
265 the SWC was after wetting, resulting in higher CO<sub>2</sub> release from the soil.

266 The total CO<sub>2</sub> released from soils (also referred to as cumulative CO<sub>2</sub> efflux) was proportional to the  
267 water retained in the soil after the wetting in both wettable and water-repellent soils (Fig. 5). The  
268 almost immediate increase in CO<sub>2</sub> efflux with wetting of sterilised soil and its return to pre-wetting

269 values after the wetting period suggests that this efflux increase has very unlikely been due to a  
270 rapid increase in microbial respiration, triggered by the reactivation of microbial activity after the  
271 sudden availability of water (Moyano et al., 2013). Several previous studies showed that the  
272 timescale for the reactivation of soil microbial activity under water-limiting conditions is a few hours  
273 (rather than seconds) after the input of water (Barnard et al., 2015; Salazar et al., 2018; Placella et  
274 al., 2012). The contribution of CO<sub>2</sub> from the chemical reaction with inorganic C (Rey, 2015) is also  
275 likely to be negligible as no inorganic C was detected in the soil. We expect that displacement of gas  
276 from soil pores by infiltrating water could be one of the sources, as suggested by Inglema et al. (2009)  
277 and Liu et al. (2002), but the amount of the cumulative efflux measured in the experiment was at  
278 least ten times higher than expected from the gas replacement. One possible mechanism  
279 responsible for the immediate CO<sub>2</sub> release after wetting may originate from the desorption of CO<sub>2</sub>  
280 molecules adsorbed to the surface of soil particles which are replaced by water molecules, as  
281 observed by Kemper et al. (1985). It has been previously suggested that the surface of SOM has the  
282 capacity to adsorb CO<sub>2</sub> (De Jonge & Mittelmeijer-Hazeleger, 1996) and that the adsorption capacity  
283 increases with the organic carbon content of the soil (Ravikovitch et al., 2005). Higher cumulative  
284 CO<sub>2</sub> effluxes measured from the soil with higher SOM content (SG soil) could thus be the result of  
285 increased adsorption capacity in comparison to CB soil. Other biochemical processes related to  
286 enzyme activity, as suggested by Fraser et al. (2015), could also have contributed to the overall CO<sub>2</sub>  
287 release.

288 Regardless of the source of the CO<sub>2</sub> it was very clear that the more water retained in the soil the  
289 higher was the cumulative CO<sub>2</sub> efflux. Unexpectedly high cumulative CO<sub>2</sub> efflux was observed with  
290 75 and 100% rewetting rates in CB-WR and, to a lesser extent, in SG-WR despite the very low  
291 retention of water upon wetting. The cumulative efflux from the water-repellent soil was  
292 significantly lower than in CB-NWR ( $p < 0.001$ ), but disproportionately high compared to the amount  
293 of retained water (Fig. 5). One possible explanation for such behaviour could be the localised  
294 increase in air pressure below the uneven wetting front (Wang et al., 2000) and along the

295 preferential flow paths (Delahaye and Alonso, 2002), which could have facilitated gas movement out  
296 of the soil.

297 While the CO<sub>2</sub> release with wetting observed in this study is short-lived, its high magnitude is in line  
298 with previous studies (Marañón-Jiménez et al., 2011; Rey et al., 2017; Sánchez-García et al., 2020). In  
299 a recent laboratory study using intact core samples, Sánchez-García et al. (2020) estimated that the  
300 CO<sub>2</sub> peak during a wetting period accounted for nearly 80% of the total CO<sub>2</sub> released over the 5 h  
301 observation period. Similarly, Marañón-Jiménez et al. (2011) estimated that the degassing of soil  
302 pores was responsible for up to 64% of the total CO<sub>2</sub> released over the 2 h following wetting. It is  
303 common that studies investigating soil surface CO<sub>2</sub> emissions inherently identify the CO<sub>2</sub> effluxes  
304 with soil respiration (Maier et al., 2011) and do not account for the storage of gas in the soil matrix.  
305 According to Maier et al. (2010) up to 20% of the soil-produced CO<sub>2</sub> is not simultaneously emitted to  
306 the atmosphere, but it is instead stored in the pore-space and released during precipitation. As it has  
307 been shown in studies by White et al. (1977) and Wang et al. (2000), air entrapment is common in  
308 dry soils and could lead to fingered flow of rainwater, but SWR could further enhance air  
309 entrapment especially during high-intensity rainfall events. Our results, which show that some of the  
310 CO<sub>2</sub> is transported downwards upon wetting, support the idea of CO<sub>2</sub> storage (air entrapment) in the  
311 soil matrix and its release at a later stage. Whereas in the bottom chamber, a significantly lower  
312 peak than in the top chamber was observed in wettable soils ( $p < 0.001$ ,  $p = 0.001$  for CB-NWR and  
313 SG-NWR respectively), in water-repellent soils, the peak in both the top and bottom chambers  
314 showed similar magnitudes ( $p = 0.525$ ,  $p = 0.184$  for CB-WR and SG-WR respectively). This downward  
315 movement of gas suggests that under natural conditions, part of the stored CO<sub>2</sub> stored might be  
316 transported downwards upon wetting towards deeper areas of the soil profile until a favourable  
317 degassing route is found.

318 Another characteristic behaviour for the release of CO<sub>2</sub> from water-repellent soils was the second  
319 CO<sub>2</sub> pulse observed with higher rewetting rates in CB-WR, but not present during the rewetting of

320 SG-WR (Fig. 2 and 3). We expect that dual porosity of soil could have led to the second peak. The  
321 first peak likely originated from the release of CO<sub>2</sub> from macropores followed by the release of gas  
322 from inside the small aggregates, which could have had different wettability characteristics  
323 compared to the bulk soil (Urbanek et al., 2007). The overall porosity was similar in soils from both  
324 sites (56 and 59% in CB and SG soils respectively), but the CB soil had a higher silt fraction and visible  
325 aggregates, still present after sample preparation, suggesting dual porosity behaviour. Pore-size  
326 distribution influences water flow through the soil matrix with larger pores facilitating rapid  
327 infiltration (Kutílek, 2004; Smith et al., 2003) and, therefore, rapid movement of CO<sub>2</sub>. The quick re-  
328 filling of larger pores first resulted in the spike observed in CB-WR, which is also supported by the  
329 quick and sharp peak (only 3 min after the start of wetting) in CB-NWR. The contribution of larger  
330 pores to the cumulative infiltration is especially pronounced in water-repellent soils, where  
331 preferential flow through larger pores has been estimated to contribute to up to 70 to 95% of the  
332 total infiltration through a water-repellent soil surface (Nyman et al., 2013). In the SG-NWR soil, the  
333 lower spike, but of longer duration (5.5 min after the start of wetting), suggests a relatively uniform  
334 re-filling of pores as a result of more homogeneous pore-size distribution.

335 This study has highlighted the substantial differences in CO<sub>2</sub> efflux upon rewetting between wettable  
336 and water-repellent soils. Given that the pre-treatment of soil material altered the internal soil  
337 structure and is likely to have affected their water flow patterns, the magnitude of the observed  
338 contrast in CO<sub>2</sub> efflux between wettable and water-repellent soils may differ somewhat to that of  
339 undisturbed field soils.

340 This study supports previous evidence that SWR potentially has a major impact on soil C dynamics  
341 (Goebel et al., 2011; Sánchez-García et al., 2020; Urbanek and Doerr, 2017), however, the effects  
342 that changes in hydrological properties caused by SWR might have on the C flux is an area that still  
343 requires further attention. Our results suggest that in highly water-repellent soils, pore-size  
344 distribution played a major role in the release of CO<sub>2</sub> after wetting, but how common this response

345 is under different factors like soil type, rainfall intensity or the degree of water repellency remains  
346 unclear.

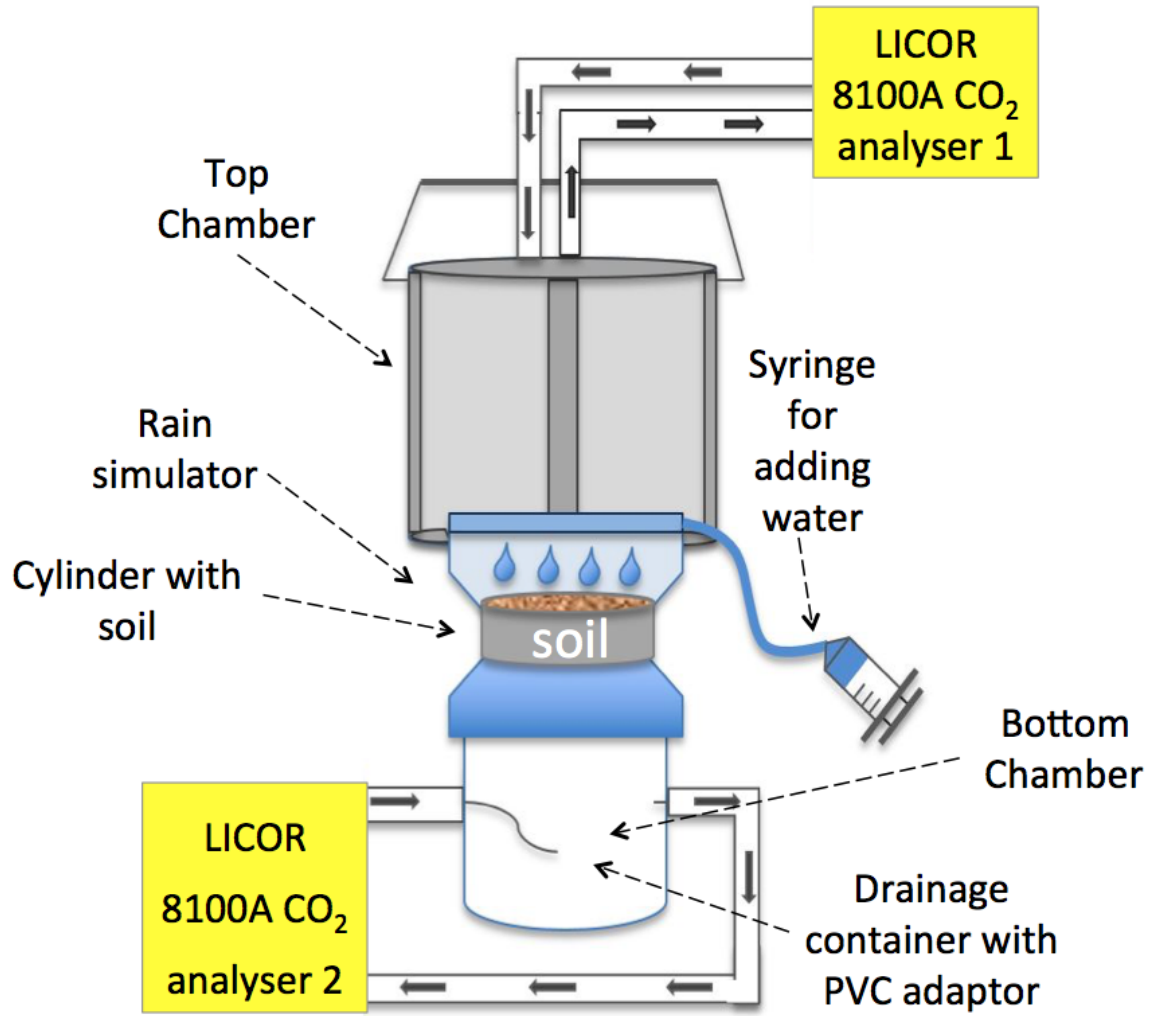
347

## 348 5. Conclusions

349 Our study shows that changes in the water-filled pore-space upon wetting, caused by SWR, reduces  
350 the short-term physical release of CO<sub>2</sub> in water-repellent soils. The high percolation concentrated  
351 along preferential paths resulted in low water retention in the soil and, therefore, low refilling of air-  
352 filled pores with infiltrating water. The CO<sub>2</sub> efflux was proportional to the amount of water retained  
353 in the soil after wetting. The pre-treatment of soil samples altered the soil structure so the CO<sub>2</sub> efflux  
354 in wettable and water-repellent soils might differ slightly in undisturbed soils. Our results also show  
355 that, upon wetting, some of the gas stored in the pore-space is displaced towards deeper areas of  
356 the soil profile and it is not released instantly. Under natural conditions, this downward flux might  
357 contribute to air entrapment below the wetting front, which could be released at a later stage.

358

359 Although SWR is a common characteristic of many soils, we are only beginning to understand the  
360 effects that water repellency-induced changes in soil hydrology might have on the overall soil C flux  
361 and current models remain unable to adequately reflect the dynamic nature of soil hydrological  
362 functions. Given that SWR is likely to become more common and severe with ongoing environmental  
363 change, future studies would be beneficial to further understand the longer-term effects of SWR on  
364 the overall soil C balance.



365  
366 Fig. 1. Schematic illustration of rewetting and CO<sub>2</sub> analyser system.

367



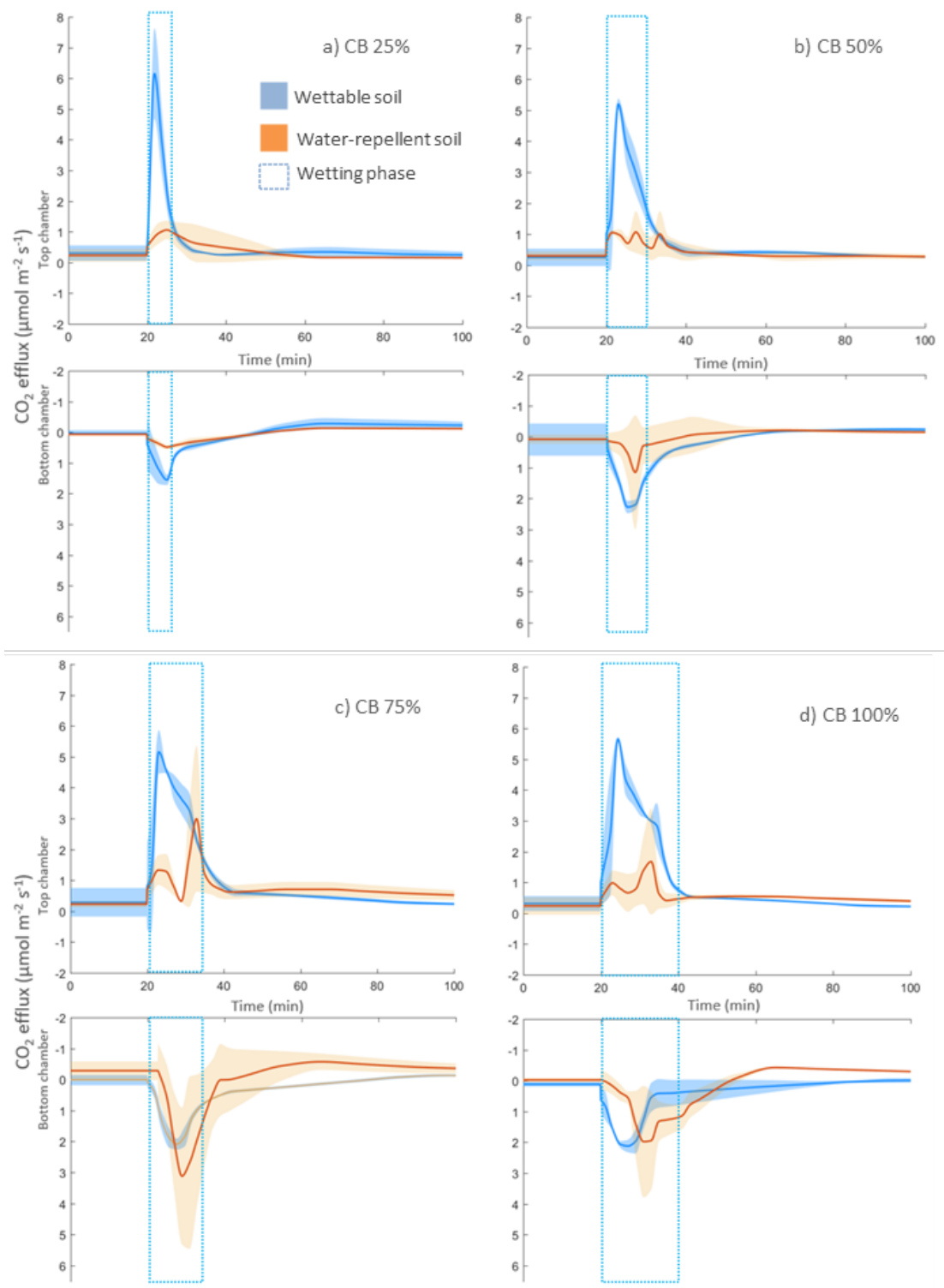


Fig. 2. Response of  $\text{CO}_2$  efflux to wetting above and below the sample for autoclaved wettable (CB-NWR) and water-repellent (CB-WR) soil from CB under the 4 different rewetting rates (% of the water-filled pore-space). The orange line and shaded area represent the mean response ( $n = 3$ ) with 95% confidence interval to the wetting of water-repellent soil and the blue line and shaded area represent the mean response ( $n = 3$ ) with 95% confidence interval to the wetting of wettable soil.

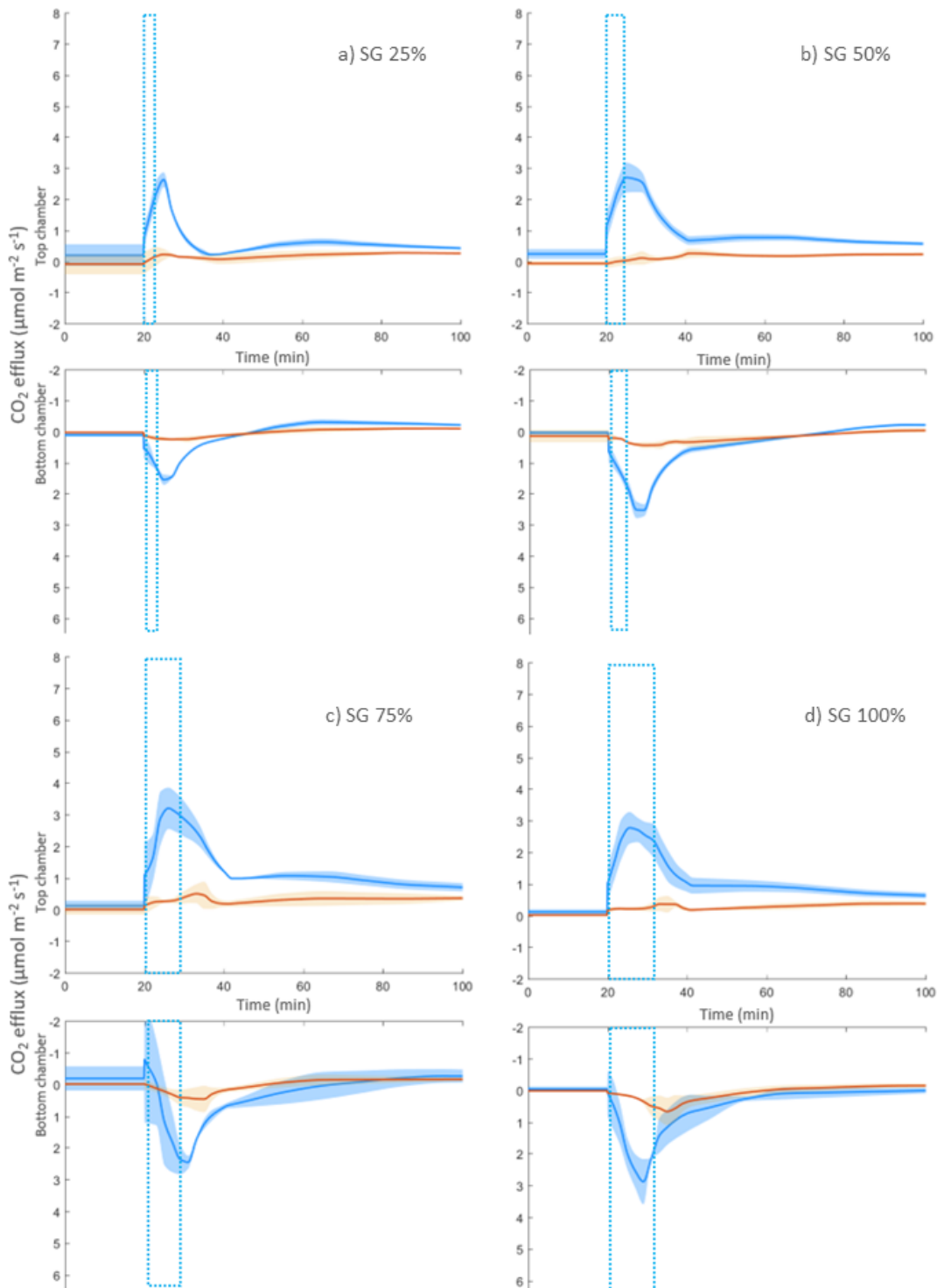
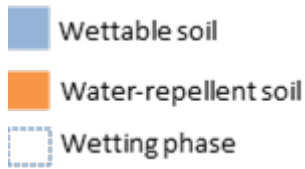


Fig. 3. Response of CO<sub>2</sub> efflux to wetting above and below the sample for autoclaved wettable (SG-NWR) and water-repellent (SG-WR) soil from SG under the 4 different rewetting rates (% of the water-filled pore-space). The orange line and shaded area represent the mean response (n = 3) with 95% confidence interval to the wetting of water-repellent soil and the blue line and shaded area represent the mean response (n = 3) with 95% confidence interval to the wetting of wettable soil.

370



Page Break

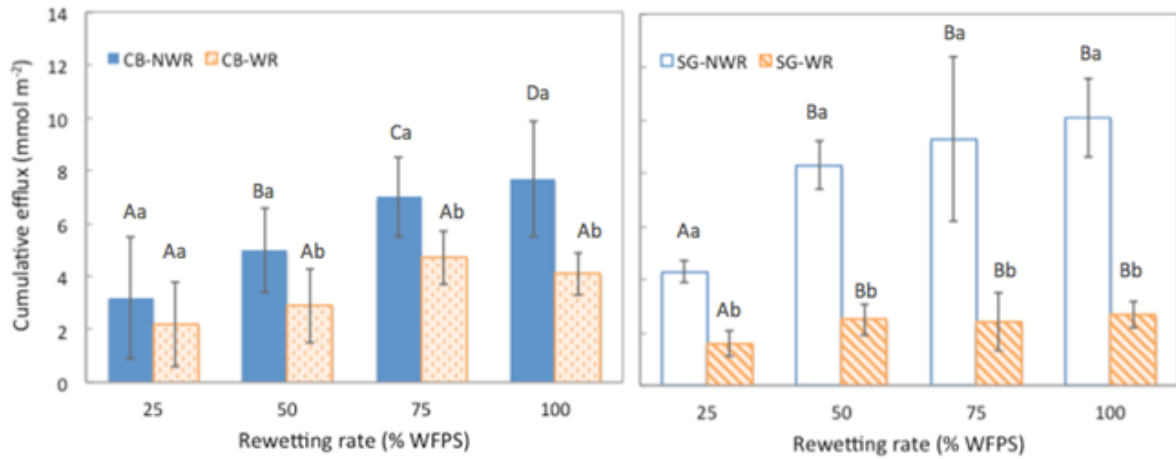


Fig. 4. Cumulative CO<sub>2</sub> efflux (top and bottom chambers combined) for wettable (CB-NWR and SG-NWR) and water-repellent (CB-WR and SG-WR) soils from CB and SG under the four different rewetting rates. Values are the mean (n = 3) with standard deviation bars. Different lowercase letters (a–b) within the same site and rewetting rate indicate significant differences between wettable and water-repellent soils at p < 0.05. Different uppercase letters (A–D) within the same site and soil wettability (wetable and water-repellent soil) indicate significant differences between rewetting rates at p < 0.05.

371

372

373

374

375

376

377

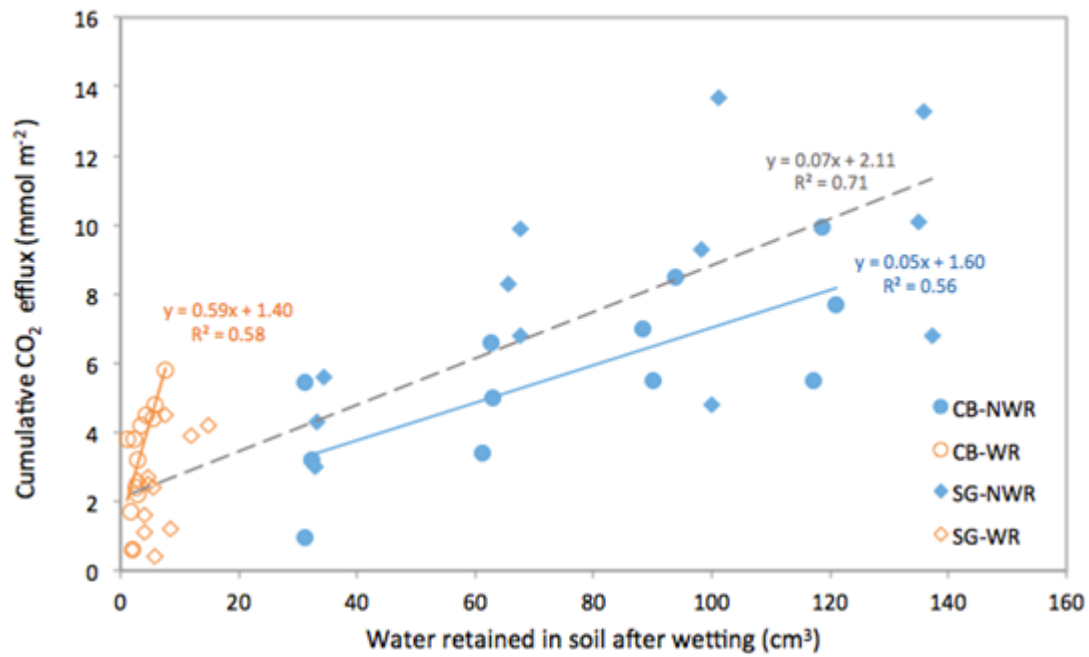


Fig. 5. Relationship between cumulative CO<sub>2</sub> efflux (top and bottom chambers combined) and water retained in the soil after wetting in wettable (CB-NWR and SG-NWR) and water-repellent (CB-WR and SG-WR) soils from CB and SG. Blue and orange solid lines represent the trendlines for CB-NWR and CB-WR respectively. The dashed line represents the trendline for the combined SG-NWR and SG-WR.

378

379

380

381

382

383

384

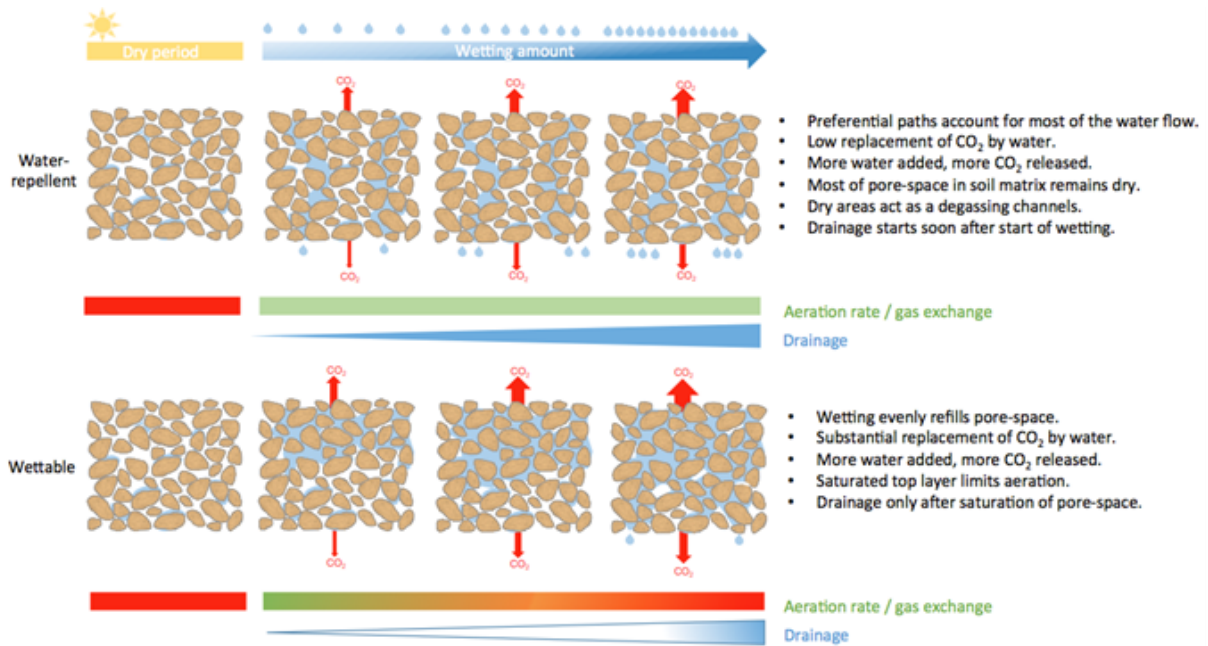


Fig. 6. Conceptual diagram of the development of wetting patterns with increasing rewetting rate in water-repellent and wettable soils and its effect on the release of CO<sub>2</sub> stored in the pore-space prior to wetting both upwards (emitted from soil surface) and downwards (contributing to CO<sub>2</sub> entrapment). Red arrows represent cumulative CO<sub>2</sub> efflux.

Table 1. General characteristics of the soils from the two study sites (CB: Cefn Bryn, SG: Southgate) before autoclaving.

	CB	SG
% Soil organic matter (SOM)	11.1 (0.4)	32.1 (0.5)
Particle density (g cm <sup>-3</sup> )	2.31 (0.1)	2 (0.1)
% Porosity	56 (1.1)	59 (2.4)
pH (H <sub>2</sub> O)	4.8 (0.06)	6.4 (0.02)
pH (CaCl <sub>2</sub> )	3.7 (0.04)	5.6 (0.02)
Particle size distribution		
% Sand	64.4 (0.03)	86.6 (1.86)
% Silt	33.6 (2.77)	12.3 (2.72)
% Clay	2.1 (0.18)	0.7 (0.17)
Texture	Sandy loam	Loamy sand

Values represent the mean (n = 3) with standard deviation in brackets.

Table 2. Soil water repellency tests results (Doerr, 1998) before and after autoclaving both soils CB and SG at air-dry, intermediate and high gravimetric soil water content (SWC) (% g g<sup>-1</sup>). Tests were done to assess optimal SWC for autoclaving to obtain wettable and water-repellent samples. Highlighted blue and pale orange values represent SWC values chosen for the experiment in order to obtain wettable and water-repellent samples respectively.

Soil	Before Autoclaving			After autoclaving			After autoclaving and oven drying (25 °C)		
	Water content (% g g <sup>-1</sup> )	WDPT (s)	SWR rating	Water content (% g g <sup>-1</sup> )	WDPT (s)	SWR rating	Water content (% g g <sup>-1</sup> )	WDPT (s)	SWR rating
CB	2.9	< 5	Wettable	6.1	256	Moderate	1.35	180	Moderate
	10.6	2120	Strong	8	> 3600	Extreme	1.28	4421	Extreme
	15.2	> 3600	Extreme	14	> 3600	Extreme	1.38	7312	Extreme
	38	< 5	Wettable	44.3	< 5	Wettable	1.57	< 5	Wettable
	49	< 5	Wettable	53.3	< 5	Wettable	1.45	< 5	Wettable
SG	4.7	< 5	Wettable	7.2	376	Moderate	3.09	423	Moderate
	11	44	Slight	14	> 3600	Extreme	3.35	8637	Extreme
	15.4	237	Moderate	19.8	> 3600	Extreme	3.42	10368	Extreme
	40.7	< 5	Wettable	40.1	11	Slight	7.1	128	Strong
	53	< 5	Wettable	52.2	< 5	Wettable	1.27	< 5	Wettable

Values represent the mean (n = 3).

Table 3. Average water retained in soil (expressed as volume in cm<sup>3</sup> and as % of total water applied) and gravimetric soil water content (SWC) (% g g<sup>-1</sup>) after wetting for autoclaved wettable and water-repellent soils from CB and SG.

Soil	Rewetting rate (%)	Water added (ml)	Wettable						Water-repellent					
			Water retained in soil (cm <sup>3</sup> )		Water retained in soil (%)		SWC (%)		Water retained in soil (cm <sup>3</sup> )		Water retained in soil (%)		SWC (%)	
CB	25	33	31.23	(0.05)	94.7	(0.07)	13.89	(0.02)	1.93	(0.85)	5.9	(0.85)	2.17	(0.34)
	50	65.5	62.33	(0.93)	95.2	(0.93)	26.33	(0.37)	3.23	(1.91)	4.9	(1.91)	2.69	(0.76)
	75	98	90.73	(2.84)	92.6	(2.84)	37.69	(1.14)	4.77	(2.63)	4.9	(2.63)	3.31	(1.05)
	100	131	118.97	(1.98)	90.8	(1.98)	48.99	(0.79)	4.1	(1.49)	3.1	(1.49)	3.04	(0.60)
SG	25	35	33.2	(0.30)	94.9	(0.3)	20	(0.15)	3.07	(1.00)	8.8	(1.0)	2.83	(0.50)
	50	70	67.27	(1.53)	96.1	(1.5)	37.03	(0.76)	6.9	(4.42)	9.9	(4.4)	4.75	(2.21)
	75	105	100.63	(2.18)	95.8	(2.2)	53.72	(1.09)	6.3	(1.23)	6	(1.2)	4.45	(0.61)
	100	140	136.53	(0.70)	97.5	(0.7)	71.67	(0.35)	9.33	(5.20)	6.7	(5.2)	5.97	(2.60)

Values represent the mean (n = 3) with standard deviation in brackets.

387

388

389

390

391



392 **Acknowledgements**

393 CSG and EU were supported by the Royal Society – Research Fellows Enhancement Award 2017  
394 (RGF\EA\180262) and Dorothy Hodgkin Fellowship (DH110189), both awarded to EU. SD was  
395 supported by NERC (grant NE/R011125/1) and OECD (contract TAD/CRP JA 95401). We would like to  
396 thank Josie Duffy for proofreading of the manuscript.

397

398 **References**

- 399 Barnard, R. L., Osborne, C. A., Firestone, M. K. (2015). Changing precipitation pattern alters soil  
400 microbial community response to wet-up under a Mediterranean-type climate. *ISME Journal*, 9,  
401 946–957. <https://doi.org/10.1038/ismej.2014.192>
- 402 Birch, H. F. (1958). The effect of soil drying on humus decomposition and nitrogen availability. *Plant*  
403 *and Soil*, 10, 9–31. <https://doi.org/10.1007/BF01343734>
- 404 Blake, G. R. (2008). Particle density. In W. Chesworth (Ed.), *Encyclopedia of Soil Science* (pp. 504–  
405 505). Dordrecht: Springer Netherlands. [https://doi.org/10.1007/978-1-4020-3995-9\\_406](https://doi.org/10.1007/978-1-4020-3995-9_406)
- 406 Borken, W., Matzner, E. (2009). Reappraisal of drying and wetting effects on C and N mineralization  
407 and fluxes in soils. *Global Change Biology*, 15, 808–824. [https://doi.org/10.1111/j.1365-](https://doi.org/10.1111/j.1365-2486.2008.01681.x)  
408 [2486.2008.01681.x](https://doi.org/10.1111/j.1365-2486.2008.01681.x)
- 409 Coumou, D., Rahmstorf, S. (2012). A decade of weather extremes. *Nature Climate Change*, 2, 491.  
410 <https://doi.org/https://doi.org/10.1038/nclimate1452>
- 411 DeBano, L. (2000). The role of fire and soil heating on water repellency in wildland environments: a  
412 review. *Journal of Hydrology*, 231–232, 195–206. [https://doi.org/10.1016/S0022-](https://doi.org/10.1016/S0022-1694(00)00194-3)  
413 [1694\(00\)00194-3](https://doi.org/10.1016/S0022-1694(00)00194-3)
- 414 Delahaye, C. H., Alonso, E. E. (2002). Soil heterogeneity and preferential paths for gas migration.

415 *Engineering Geology*, 64, 251–271. [https://doi.org/10.1016/S0013-7952\(01\)00104-1](https://doi.org/10.1016/S0013-7952(01)00104-1)

416 de Jonge, H., Mittelmeijer-Hazeleger, M. C. (1996). Adsorption of CO<sub>2</sub> and N<sub>2</sub> on soil organic matter:  
417 Nature of porosity, surface area, and diffusion mechanisms. *Environmental Science and*  
418 *Technology*, 30, 408–413. <https://doi.org/10.1021/es950043t>

419 de Nijs, E. A., Hicks, L. C., Leizeaga, A., Tietema, A., Rousk, J. (2018). Soil microbial moisture  
420 dependences and responses to drying-rewetting: the legacy of 18 years drought. *Global Change*  
421 *Biology*, 0–2. <https://doi.org/10.1111/gcb.14508>

422 Doerr, S. H., Shakesby, R. A., Walsh, R. P. D. (2000). Soil water repellency: Its causes, characteristics  
423 and hydro-geomorphological significance. *Earth Science Reviews*, 51, 33–65.  
424 [https://doi.org/10.1016/S0012-8252\(00\)00011-8](https://doi.org/10.1016/S0012-8252(00)00011-8)

425 Doerr, S. H. (1998). On standardizing the ‘Water Drop Penetration Time’ and the ‘Molarity of an  
426 Ethanol Droplet’ techniques to classify soil hydrophobicity: a case study using medium textured  
427 soils. *Earth Surface Processes and Landforms*, 23, 663–668. [https://doi.org/10.1002/\(SICI\)1096-](https://doi.org/10.1002/(SICI)1096-9837(199807)23:7<663::AID-ESP909>3.0.CO;2-6)  
428 [9837\(199807\)23:7<663::AID-ESP909>3.0.CO;2-6](https://doi.org/10.1002/(SICI)1096-9837(199807)23:7<663::AID-ESP909>3.0.CO;2-6)

429 Doerr, S. H., Ferreira, A. J. D., Walsh, R. P. D., Shakesby, R. A., Leighton-Boyce, G., Coelho, C. O. A.  
430 (2003). Soil water repellency as a potential parameter in rainfall-runoff modelling:  
431 experimental evidence at point to catchment scales from Portugal. *Hydrological Processes*, 17,  
432 363–377. <https://doi.org/10.1002/hyp.1129>

433 Doerr, S. H., Thomas, A. (2000). The role of soil moisture in controlling water repellency: new  
434 evidence from forest soils in Portugal. *Journal of Hydrology*, 231, 134–147.  
435 [https://doi.org/10.1016/S0022-1694\(00\)00190-6](https://doi.org/10.1016/S0022-1694(00)00190-6)

436 Fraser, F. C., Corstanje, R., Deeks, L. K., Harris, J. A., Pawlett, M., Todman, L. C., Whitmore, A. P., Ritz,  
437 K. (2016). On the origin of carbon dioxide released from rewetted soils. *Soil Biology and*  
438 *Biochemistry*, 101, 1–5. <https://doi.org/10.1016/j.soilbio.2016.06.032>

439 Goebel, M. O., Bachmann, J., Reichstein, M., Janssens, I. A., Guggenberger, G. (2011). Soil water  
440 repellency and its implications for organic matter decomposition - is there a link to extreme  
441 climatic events? *Global Change Biology*, 17, 2640–2656. [https://doi.org/10.1111/j.1365-](https://doi.org/10.1111/j.1365-2486.2011.02414.x)  
442 2486.2011.02414.x

443 Goebel, M.-O., Woche, S. K., Bachmann, J. (2012). Quantitative analysis of liquid penetration kinetics  
444 and slaking of aggregates as related to solid–liquid interfacial properties. *Journal of Hydrology*,  
445 442–443, 63–74. <https://doi.org/10.1016/J.JHYDROL.2012.03.039>

446 Goebel, M. O., Woche, S. K., Bachmann, J., Lamparter, A., Fischer, W. R. (2007). Significance of  
447 wettability-induced changes in microscopic water distribution for soil organic matter  
448 decomposition. *Soil Science Society of America Journal*, 71, 1593–1599.  
449 <https://doi.org/doi:10.2136/sssaj2006.0192>

450 Göransson, H., Godbold, D. L., Jones, D. L., Rousk, J. (2013). Bacterial growth and respiration  
451 responses upon rewetting dry forest soils: Impact of drought-legacy. *Soil Biology and*  
452 *Biochemistry*, 57, 477–486. <https://doi.org/10.1016/j.soilbio.2012.08.031>

453 Hendrickx, J. M. H., Flury, M. (2001). Uniform and preferential flow mechanisms in the vadose zone.  
454 In *Conceptual models of flow and transport in the fractured vadose zone*. (pp. 149–187).  
455 Washington, DC: Natl.Acad.Press.

456 Huxman, T., Snyder, K., Tissue, D., Leffler, A. J., Ogle, K., Pockman, W., Sandquist, D. R., Potts, D. L.,  
457 Schwinning, S. (2004). Precipitation pulses and carbon fluxes in semiarid and arid ecosystems.  
458 *Oecologia*, 141, 254–268. <https://doi.org/10.1007/s00442-004-1682-4>

459 Inglima, I., Alberti, G., Bertolini, T., Vaccari, F. P., Gioli, B., Miglietta, F., Cotrufo, M. F., Peressotti, A.  
460 (2009). Precipitation pulses enhance respiration of Mediterranean ecosystems: the balance  
461 between organic and inorganic components of increased soil CO<sub>2</sub> efflux. *Global Change Biology*,  
462 15, 1289–1301. <https://doi.org/10.1111/j.1365-2486.2008.01793.x>

463 Kim, D. G., Vargas, R., Bond-Lamberty, B., Turetsky, M. R. (2012). Effects of soil rewetting and  
464 thawing on soil gas fluxes: a review of current literature and suggestions for future research.  
465 *Biogeosciences*, 9, 2459–2483. <https://doi.org/10.5194/bg-9-2459-2012>

466 Kutílek, M. (2004). Soil hydraulic properties as related to soil structure. *Soil and Tillage Research*, 79,  
467 175–184. <https://doi.org/10.1016/j.still.2004.07.006>

468 Lado-Monserrat, L., Lull, C., Bautista, I., Lidón, A., Herrera, R. (2014). Soil moisture increment as a  
469 controlling variable of the “Birch effect”. Interactions with the pre-wetting soil moisture and  
470 litter addition. *Plant and Soil*, 379, 21–34. <https://doi.org/10.1007/s11104-014-2037-5>

471 Lamparter, A., Bachmann, J., Goebel, M.-O., Woche, S. K. (2009). Carbon mineralization in soil:  
472 Impact of wetting–drying, aggregation and water repellency. *Geoderma*, 150, 324–333.  
473 <https://doi.org/10.1016/j.geoderma.2009.02.014>

474 Leon, E., Vargas, R., Bullock, S., Lopez, E., Rodrigo, A., La, N., Jr, S. (2014). Hot spots, hot moments,  
475 and spatio-temporal controls on soil CO<sub>2</sub> efflux in a water-limited ecosystem. *Soil Biology and*  
476 *Biochemistry*, 77, 12–21. <https://doi.org/10.1016/j.soilbio.2014.05.029>

477 Liu, X., Wan, S., Su, B., Hui, D., Luo, Y. (2002). Response of soil CO<sub>2</sub> efflux to water manipulation in a  
478 tallgrass prairie ecosystem. *Plant and Soil*, 240, 213–223.  
479 <https://doi.org/https://doi.org/10.1023/A:1015744126533>

480 LI-COR. (2010). Using the LI-8100A Soil Gas Flux System and the LI-8150 Multiplexer. LI-COR, Inc.  
481 Retrieved from [www.licor.com/env](http://www.licor.com/env)

482 Maier, M., Schack-Kirchner, H., Hildebrand, E. E., Holst, J. (2010). Pore-space CO<sub>2</sub> dynamics in a deep,  
483 well-aerated soil. *European Journal of Soil Science*, 61, 877–887.  
484 <https://doi.org/10.1111/j.1365-2389.2010.01287.x>

485 Maier, M., Schack-Kirchner, H., Hildebrand, E. E., Schindler, D. (2011). Soil CO<sub>2</sub> efflux vs. soil  
486 respiration: implications for flux models. *Agricultural and Forest Meteorology*, 151, 1723–1730.

487 <https://doi.org/10.1016/j.agrformet.2011.07.006>

488 Marañón-Jiménez, S., Castro, J., Kowalski, A. S., Serrano-Ortiz, P., Reverter, B. R., Sánchez-Cañete, E.  
489 P., Zamora, R. (2011). Post-fire soil respiration in relation to burnt wood management in a  
490 Mediterranean mountain ecosystem. *Forest Ecology and Management*, 261, 1436–1447.  
491 <https://doi.org/10.1016/j.foreco.2011.01.030>

492 Meisner, A., Leizeaga, A., Rousk, J., Bååth, E. (2017). Partial drying accelerates bacterial growth  
493 recovery to rewetting. *Soil Biology and Biochemistry*, 112, 269–276.  
494 <https://doi.org/10.1016/j.soilbio.2017.05.016>

495 Meisner, A., Rousk, J., Bååth, E. (2015). Prolonged drought changes the bacterial growth response to  
496 rewetting. *Soil Biology and Biochemistry*, 88, 314–322.  
497 <https://doi.org/10.1016/j.soilbio.2015.06.002>

498 Moyano, F. E., Manzoni, S., Chenu, C. (2013). Responses of soil heterotrophic respiration to moisture  
499 availability: An exploration of processes and models. *Soil Biology and Biochemistry*, 59, 72–85.  
500 <https://doi.org/10.1016/j.soilbio.2013.01.002>

501 Muhr, J., Borken, W. (2009). Delayed recovery of soil respiration after wetting of dry soil further  
502 reduces C losses from a Norway spruce forest soil. *Journal of Geophysical Research*, 114,  
503 G04023. <https://doi.org/10.1029/2009JG000998>

504 Muhr, J., Goldberg, S. D., Borken, W., Gebauer, G. (2008). Repeated drying-rewetting cycles and their  
505 effects on the emission of CO<sub>2</sub>, N<sub>2</sub>O, NO, and CH<sub>4</sub> in a forest soil. In *Journal of Plant Nutrition*  
506 *and Soil Science*, 171, 719-728. <https://doi.org/10.1002/jpln.200700302>

507 Müller, K., Deurer, M., Kawamoto, K., Kuroda, T., Subedi, S., Hiradate, S., Komatsu, T., Clothier, B. E.  
508 (2014). A new method to quantify how water repellency compromises soils' filtering function.  
509 *European Journal of Soil Science*, 65, 348–359. <https://doi.org/10.1111/ejss.12136>

510 Nelson, D. W., Sommers, L. E. (1996). Total Carbon, Organic Carbon, and Organic Matter. In *Methods*

511 *of Soil Analysis* (SSSA Book, pp. 961–1010). Madison, WI: SSSA and ASA.

512 Norman, J. M., Garcia, R., Verma, S. B. (1992). Soil surface CO<sub>2</sub> fluxes and the carbon budget of a  
513 grassland. *Journal of Geophysical Research: Atmospheres*, *97*, 18845–18853.  
514 <https://doi.org/10.1029/92JD01348>

515 Nyman, P., Sheridan, G., Smith, H., Lane, P. (2013). Modeling the effects of surface storage,  
516 macropore flow and water repellency on infiltration after wildfire. *Journal of Hydrology*, *513*,  
517 301–313. <https://doi.org/10.1016/J.JHYDROL.2014.02.044>

518 Placella, S. A., Brodie, E. L., Firestone, M. K. (2012). Rainfall-induced carbon dioxide pulses result  
519 from sequential resuscitation of phylogenetically clustered microbial groups. *Proceedings of the*  
520 *National Academy of Sciences of the United States of America*, *109*, 10931–10936.  
521 <https://doi.org/10.1073/pnas.1204306109>

522 Ravikovitch, P. I., Bogan, B. W., Neimark, A. V. (2005). Nitrogen and carbon dioxide adsorption by  
523 soils. *Environmental Science and Technology*, *39*, 4990–4995.  
524 <https://doi.org/10.1021/es048307b>

525 Rey, A. (2015). Mind the gap: non-biological processes contributing to soil CO<sub>2</sub> efflux. *Global Change*  
526 *Biology*, *21*, 1752–1761. <https://doi.org/10.1111/gcb.12821>

527 Rey, A., Oyonarte, C., Morán-López, T., Raimundo, J., Pegoraro, E. (2017). Changes in soil moisture  
528 predict soil carbon losses upon rewetting in a perennial semiarid steppe in SE Spain. *Geoderma*,  
529 *287*, 135–146. <https://doi.org/10.1016/j.geoderma.2016.06.025>

530 Ritsema, C. J., Dekker, L. W. (1994). How water moves in a water repellent sandy soil: 2. Dynamics of  
531 fingered flow. *Water Resour. Res.*, *30*, 2519–2531.

532 Ritsema, C. J., Dekker, L. W. (2000). Preferential flow in water repellent sandy soils: principles and  
533 modeling implications. *Journal of Hydrology*, *231–232*, 308–319.  
534 [https://doi.org/10.1016/S0022-1694\(00\)00203-1](https://doi.org/10.1016/S0022-1694(00)00203-1)

535 Robinson, D. A., Hopmans, J. W., Filipovic, V., van der Ploeg, M., Lebron, I., Jones, S. B., Reinsch, S.,  
536 Jarvis, N., Tuller, M. (2019). Global environmental changes impact soil hydraulic functions  
537 through biophysical feedbacks. *Global Change Biology*, 25, 1895–1904.  
538 <https://doi.org/10.1111/gcb.14626>

539 Salazar, A., Sulman, B. N., Dukes, J. S. (2018). Microbial dormancy promotes microbial biomass and  
540 respiration across pulses of drying-wetting stress. *Soil Biology and Biochemistry*, 116, 237–244.  
541 <https://doi.org/10.1016/j.soilbio.2017.10.017>

542 Sánchez-García, C., Oliveira, B. R. F., Keizer, J. J., Doerr, S. H., Urbanek, E. (2020). Water repellency  
543 reduces soil CO<sub>2</sub> efflux upon rewetting. *Science of The Total Environment*, 708, 135014.  
544 <https://doi.org/10.1016/J.SCITOTENV.2019.135014>

545 Schimel, J. P. (2018). Life in Dry Soils: Effects of Drought on Soil Microbial Communities and  
546 Processes. *Annual Review of Ecology, Evolution, and Systematics*, 49, 409–432.  
547 <https://doi.org/10.1146/annurev-ecolsys-110617-062614>

548 Schymanski, S., Grahm, L., Or, D. (2017). The physical origins of rapid soil CO<sub>2</sub> release following  
549 wetting. Presented at the EGU General Assembly 23-28 April 2017, Vienna.

550 Seaton, F. M., Jones, D. L., Creer, S., George, P. B. L., Smart, S. M., Lebron, I., Barret, G., Emmett, B.  
551 A., Robinson, D. A. (2019). Plant and soil communities are associated with the response of soil  
552 water repellency to environmental stress. *Science of The Total Environment*, 687, 929–938.  
553 <https://doi.org/10.1016/J.SCITOTENV.2019.06.052>

554 Smith, A. P., Bond-Lamberty, B., Benscoter, B. W., Tfaily, M. M., Hinkle, C. R., Liu, C., Bailey, V. L.  
555 (2017). Shifts in pore connectivity from precipitation versus groundwater rewetting increases  
556 soil carbon loss after drought. *Nature Communications*, 8, 1–11.  
557 <https://doi.org/10.1038/s41467-017-01320-x>

558 Smith, K. A., Ball, T., Conen, F., Dobbie, K. E., Massheder, J., Rey, A. (2003). Exchange of  
559 greenhousegases between soil and atmosphere: interactions of soil physical factors and

560 biological processes. *European Journal of Soil Science*, 54, 779–791.  
561 <https://doi.org/10.1046/j.1365-2389.2003.00567.x>

562 Sponseller, R. A. (2007). Precipitation pulses and soil CO<sub>2</sub> flux in a Sonoran Desert ecosystem. *Global*  
563 *Change Biology*, 13, 426–436. <https://doi.org/10.1111/j.1365-2486.2006.01307.x>

564 Trenberth, K. E., Dai, A., van der Schrier, G., Jones, P. D., Barichivich, J., Briffa, K. R., Sheffield, J.  
565 (2013). Global warming and changes in drought. *Nature Climate Change*, 4, 17.  
566 <https://doi.org/https://doi.org/10.1038/nclimate2067>

567 Urbanek, E., Bodi, M., Doerr, S. H., Shakesby, R. A. (2010). Influence of Initial Water Content on the  
568 Wettability of Autoclaved Soils. *Soil Science Society of America Journal*, 74, 2086–2088.  
569 <https://doi.org/10.2136/sssaj2010.0164N>

570 Urbanek, E., Doerr, S. H. (2017). CO<sub>2</sub> efflux from soils with seasonal water repellency.  
571 *Biogeosciences*, 14, 4781–4794. <https://doi.org/https://doi.org/10.5194/bg-14-4781-2017>

572 Urbanek, E., Hallett, P., Feeney, D., Horn, R. (2007). Water repellency and distribution of hydrophilic  
573 and hydrophobic compounds in soil aggregates from different tillage systems. *Geoderma*, 140,  
574 147–155. <https://doi.org/10.1016/j.geoderma.2007.04.001>

575 Urbanek, E., Shakesby, R. A. (2009). Impact of stone content on water movement in water-repellent  
576 sand. *European Journal of Soil Science*, 60, 412–419. [https://doi.org/10.1111/j.1365-](https://doi.org/10.1111/j.1365-2389.2009.01128.x)  
577 [2389.2009.01128.x](https://doi.org/10.1111/j.1365-2389.2009.01128.x)

578 Urbanek, E., Walsh, R. P. D., Shakesby, R. A. (2015). Patterns of soil water repellency change with  
579 wetting and drying: The influence of cracks, roots and drainage conditions. *Hydrological*  
580 *Processes*, 29, 2799–2813. <https://doi.org/10.1002/hyp.10404>

581 Wang, Z., Wu, Q., Wu, L., Ritsema, C., Dekker, L., Feyen, J. (2000). Effects of soil water repellency on  
582 infiltration rate and flow instability. *Journal of Hydrology*, 231–232, 265–276.  
583 [https://doi.org/10.1016/S0022-1694\(00\)00200-6](https://doi.org/10.1016/S0022-1694(00)00200-6)



584 Waring, B. G., Powers, J. S. (2016). Unraveling the mechanisms underlying pulse dynamics of soil  
585 respiration in tropical dry forests. *Environmental Research Letters*, 11.  
586 <https://doi.org/10.1088/1748-9326/11/10/105005>

587 White, I., Colombero, P. M., Philip, J. R. (1977). Experimental Studies of Wetting Front Instability  
588 Induced by Gradual Change of Pressure Gradient and by Heterogeneous Porous Media1. *Soil*  
589 *Science Society of America Journal*, 41, 483–489.  
590 <https://doi.org/10.2136/sssaj1977.03615995004100030010x>

591 Wofford, P., Vidrio, E. (2015). *Procedure for Determining Soil Particle Density Using Gay-Lussac*  
592 *Specific-Gravity Bottles*. Sacramento.

593